

## VORTICAL STRUCTURES AND PARTICLES IN RAYLEIGH-BÉNARD CONVECTION

**Sangro Park**

Department of Computational Science and Engineering  
Yonsei University  
50 Yonsei-ro Seodaemun-gu  
psr4109@naver.com

**Changhoon Lee**

Department of Computational Science and Engineering & Department of Mechanical Engineering  
Yonsei University  
50 Yonsei-ro Seodaemun-gu  
clee@yonsei.ac.kr

### ABSTRACT

Behavior of vortical structures and particle dispersion in Rayleigh-Bénard convection is investigated by direct numerical simulation using a spectral method. The flow regime is soft turbulence with Rayleigh number of  $10^6$ , Prandtl number 0.7 and the aspect ratio 6 : 1 : 6. Simulation reveals that the horizontal vorticity occurring near the wall and at the border of thermal plumes affect dynamics of thermal plumes significantly. Vortical natures of thermal plumes are examined through the invariants of velocity gradient tensor. Inhomogeneous distribution of particles only affected by fluid motions (one-way coupling) is also investigated using the point particle approach for Stokes number 0.1, 1, 5 and 20.

### Introduction

Rayleigh-Bénard convection has a simple geometry so that the flow parameters can be easily controlled, while it consists of various thermal flow dynamics. For this reason, many studies have focused on the global quantities such as Nusselt number and its relation with flow parameters and geometry. Additionally, structures are known to affect the Rayleigh and Prandtl number scaling so that many studies on visualization of the structures and physical properties of thermal structures have already been carried out. The predominant structures near the wall, in which large thermal gradient and conduction heat flux exist, are thermal and line plumes. Thermals are hot/cold fluid blobs released and detached from the boundary layer. Krishnamurti & Howard (1981) modeled the near-wall dynamics as a periodic growth of conduction layer by diffusion, which becomes unstable and releases thermals when Rayleigh number based on the conduction layer thickness becomes about 1000; then new conduction layer begins to form and grow. Line plumes are structures which release hot/cold fluid from lines continuously. They move randomly in space and merge with one another. Zocchi *et al.* (1990) visualized propagating line plumes near the

wall in experiments and explained life cycles of coherent structures at the boundary layer where they strike the wall and excite waves. The waves propagate the line plumes which merge and release thermals to the opposite wall. The physical properties of thermal plumes such as local heat flux and thermal dissipation rate were studied by (Shishkina & Wagner (2006); Shishkina & Wagner (2007); Shishkina & Wagner (2008)). Inside the thermal plumes, local heat flux, and vertical component of vorticity are large. In contrast, heat flux value and thermal dissipation rate is small in background region. At the border of the thermal plume, thermal dissipation rate is large and horizontal components of vorticity become large. On the other hand, the vortical structures have been studied by the eigenvalues and invariants of velocity gradient tensor and strain/rotation rate tensor for isotropic and channel turbulent flows, but not in Rayleigh-Bénard convection. (Ooi *et al.* (1999); Blackburn *et al.* (1996))

For the past few decades, the vast majority of studies of Rayleigh-Bénard convection have been addressing the single phase cases. However, multiphase thermal convection deserves to be focused as a fundamental study of physics and as a practical application in industry, weather prediction, etc. As a representative study of particle simulation study in Rayleigh-Bénard convection, Oresta & Prosperetti (2013) investigated thermal, mechanical and combined coupling of fluid and particle motions in slender cylinder. They revealed the effect of particles on heat flux and turbulence intensity in thermal convection. Particle studies in Rayleigh-Bénard convection in a long cylinder with relation to thermal structures are carried out in Oresta *et al.* (2006). They investigated the invariants of velocity gradient tensor at particle locations, and showed the features in particle accumulation regions. Although studies of particle behavior in turbulence are vigorously conducted in various geometries like pipe, channel and isotropic domains (Rouson & Eaton (2001); Elghobashi (1994)), particle studies in natural convection in a wide plane domain is rare.

In this study, we mainly investigate the relation be-

tween vortical structures and thermal plumes by focusing on vertical stretching and horizontal shear near the wall. Additionally, we investigated the topology of vortical structures with joint probability density functions of invariants of velocity gradient tensor. For the particle simulation we considered the effect of fluid to particle motion (one-way coupling) using the point particle approach. The simulation results include time averaged concentration of particles of various Stokes number in the vertical locations in the domain.

## Numerical Approach

Rayleigh-Bénard convection is defined as flow confined between hot lower boundary wall and cold upper one. In this study, the dimensions of horizontal ( $x$ -,  $z$ -) and vertical( $y$ -) directions are  $L_x : L_y : L_z = 6 : 1 : 6$ . Constant temperatures and no-slip velocity conditions are used at boundary walls and periodic boundary conditions for side walls. A spectral method with dealiased Fourier and Chebyshev expansions in the horizontal and vertical directions are used to solve the governing equation. The Crank-Nicolson method and a 3rd-order Runge-Kutta schemes are applied for time advancing of the viscous terms and nonlinear terms including buoyant source, respectively. The governing equations are non-dimensionalized by using  $\kappa/H$ ,  $H$ ,  $\Delta T (= 2T_w)$ , where  $\kappa$ ,  $H$ ,  $\Delta T$ ,  $T_w$  are thermal conductivity, domain height, temperature difference, wall temperature, respectively. The non-dimensional governing equations are

$$\frac{\partial u_i}{\partial x_i} = 0 \quad (1)$$

$$\frac{\partial u_i}{\partial t} + u_j \frac{\partial u_i}{\partial x_j} = -\frac{\partial p}{\partial x_i} + Pr \frac{\partial^2 u_i}{\partial x_j \partial x_j} + Ra Pr T' \delta_{i2} \quad (2)$$

$$\frac{\partial T}{\partial t} + u_j \frac{\partial T}{\partial x_j} = \frac{\partial^2 T}{\partial x_j \partial x_j} \quad (3)$$

In equation (2), Rayleigh and Prandtl numbers are defined as  $Ra = (\beta g H^3 \Delta T) / (\kappa \nu)$ ,  $Pr = \nu / \kappa$  and  $\beta$ ,  $\nu$  are thermal expansion coefficient and kinematic viscosity.

A one-way particle tracking algorithm is coupled with fluid governing equations to calculate particle trajectories in the flow field using the 4th-order Hermite interpolation combined with 6th-order Lagrangian polynomial. With the known fluid velocity at particle position, the equations of particle motions are integrated employing a 3rd-order Runge-Kutta scheme. The dimensional governing equation of particles (ignoring gravity effect) are

$$\frac{d\mathbf{v}}{dt} = \frac{f(Re_p)}{\tau_p} (\mathbf{u} - \mathbf{v}) \quad (4)$$

In the equation, the particle Reynolds number is defined as  $Re_p = (d_p |\mathbf{v} - \mathbf{u}|) / \nu$ , where  $d_p$ ,  $\mathbf{v}$ ,  $\mathbf{u}$  are particle diameter, particle velocity, and fluid velocity at particle location.  $\tau_p$  is the particle response time defined as  $(\rho_p d_p^2) / (18 \rho \nu)$ . Stokes numbers  $St_k$ , the ratio of particle response time to the Komogorov time scale, are 0.1, 1, 5 and 20 in our simulations.

## Invariant analysis of vortical structures

Flow domain is divided into three regions (boundary layer, plume mixing layer and central region), which show distinguishing behaviors. Inside the thermal boundary layer, conductive heat transport is dominant mechanism. Due to the horizontally moving sheet-like plumes, horizontal shear is large, which makes horizontal stretching of fluid element. Central region covers mid-plane and shows nearly isothermal behaviors. At the thermal plume mixing layer, flows from boundary layer matches to the central region. In this paper, the three regions are classified based on the vertical distribution of mean temperature and vertical acceleration. Inside boundary layer region is located at  $0 < y < \delta_T/H (= 0.0375)$ , plume mixing layer is  $0.04 < y < 0.3$ , and the central region is at  $0.3 < y < 0.5$  for the lower half region of the whole flow domain.

Velocity gradient tensor,  $A_{ij} = \partial u_i / \partial x_j$  has the characteristic equation given by

$$\lambda_i^3 + P_A \lambda_i^2 + Q_A \lambda_i + R_A = 0 \quad (5)$$

Here  $\lambda_i$  is eigenvalue and the invariants can be derived as following equations.

$$P_A = A_{ii} \quad (6)$$

$$Q_A = -\frac{1}{2} A_{ij} A_{ji} \quad (7)$$

$$R_A = -\frac{1}{3} A_{ij} A_{jk} A_{ki} \quad (8)$$

$$D_A = \frac{27}{4} R_A^2 + Q_A^3 \quad (9)$$

The joint probability density functions of the invariants shows the topology of the local vortical structures. Figure 1 illustrates the joint probability density functions between  $R_A$  and  $Q_A$  inside thermal boundary layer and central regions. SF/S, UF/C indicate stable focus/stretching, unstable focus/contraction at positive determinant region ( $D_A > 0$ ). SN/S/S, UN/S/S mean stable node/saddle/saddle, unstable node/saddle/saddle at negative determinant region. Like other turbulent flows, zero at the origin is the most probable value and shows preference along  $D_A = 0$  line in fourth quadrant, which indicates most of the largely strained eddies show near-vortical motion, i.e., predominance of vortex stretching. Near the wall, the probability in region of  $D_A < 0$  increases. These regions are convergence regions, i.e., along two principal axes flow converges and flow diverges in the other axis. This seems to be attributed to wave propagation from thermal plumes. The shapes of joint probability density functions at different regions of Rayleigh-Bénard convection are mostly affected by thermal plume activities. As explained in Zocchi *et al.* (1990), vertically moving thermal plumes make spreading and concentration of fluid at boundary layer regions by striking the wall, therefore horizontally propagating sheet-like thermal structures are dominant at boundary regions as shown by preference to UN/S/S region in figure 1 (a). Although vertical movements of thermal plumes, nearly isothermal behavior is shown in the central region because of mixing. The result is pear-shaped distribution of joint PDF in central region which is similar to that in isotropic turbulence.

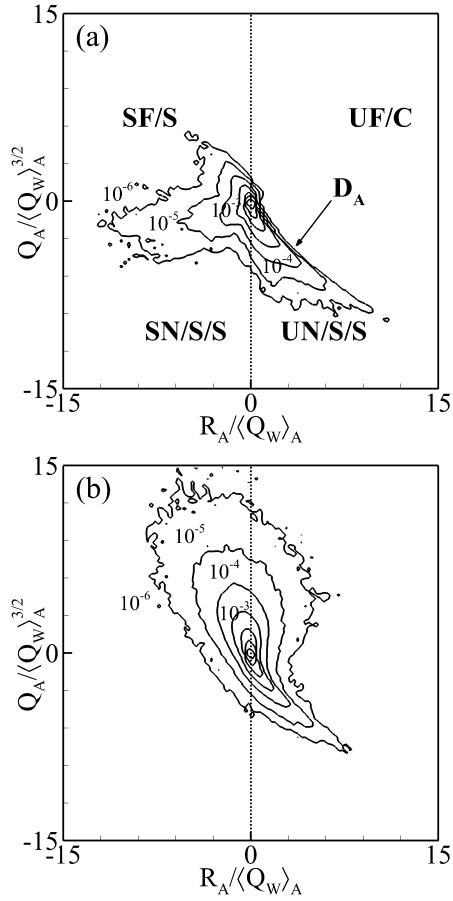


Figure 1. Distribution of joint probability density functions of  $R_A$ ,  $Q_A$  at (a):  $y < \delta_T/H$  ( $y = 0.02$ ), (b):  $y = 0.5$ .

### Inhomogeneous distribution of particles

Most studies about particle simulations of wall bounded turbulence have been focusing on fully developed channel or pipe flows. The most significant turbulent coherent structures that affect momentum, heat, and mass transfer are vortical structures near the wall Soldati (2005). The wall vortical structures are known to change particle accumulation by ejection and sweep motions. However, the dominant coherent structure in natural convection is thermal plumes which affect particle concentration and motions of fluid. Effect of temperature in natural convection on particle diffusion is discussed in Elperin *et al.* (1996) by studying the relations of particle flux and thermal diffusion. Pallares & Grau (2012) studied the particle dispersion and concentration in turbulent natural convection flow between two vertical walls at Stokes number from 0.843 to 17.45, in which different characteristics of deposition velocities with gravitational force were discussed. In our simulation, number of particles are 500,000, the density ratio of particle to fluid is 833, which is a practical value of a droplet in the air, but we ignored the gravitational effect on particles which was considered Pallares & Grau (2012). Values used in the simulation are shown in table 1.

We started our simulation from uniform distribution of particles in the whole domain. As time goes, particle distributions become nonuniform. Figure 2 includes change of particle concentration from uniform distribution at Stokes numbers 0.1, 1, 5 and 20. The concentration is defined as

Table 1. Summary of particle properties used in the simulations (normalized with domain half height,  $H/2$  and thermal conductivity,  $\kappa$ )

St	$\tau_p \kappa / (H^2/4)$	$d_p / (H/2)$	$\rho_p / \rho$
0.1	0.000108	0.001277	833
1	0.001079	0.004	833
5	0.005393	0.009032	833
20	0.021573	0.018064	833

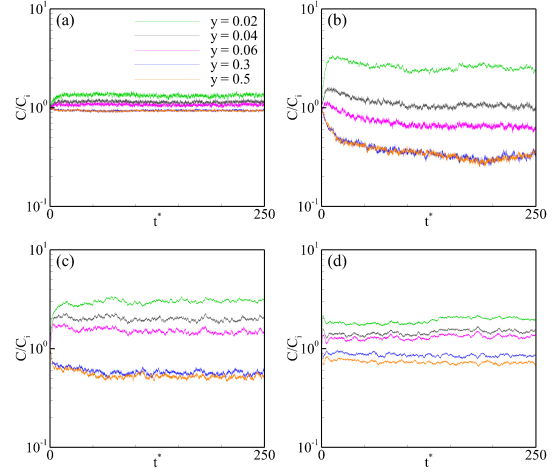


Figure 2. Change of particle concentration with time at Stokes number (a) 0.1, (b) 1, (c) 5 and (d) 20.

number of particles per unit volume at a specific vertical location normalized by the initial number of particles at the same vertical location ( $C/C_i$ ). The change of concentration of particles in time shows the accumulation of particles at specific vertical locations, implying the preferential concentration, particularly at Stokes numbers 1 and 5. Since particles follow small-scale fluid motion at Stokes number 0.1, the concentration of particles does not change significantly after a long time. For the largest Stokes number

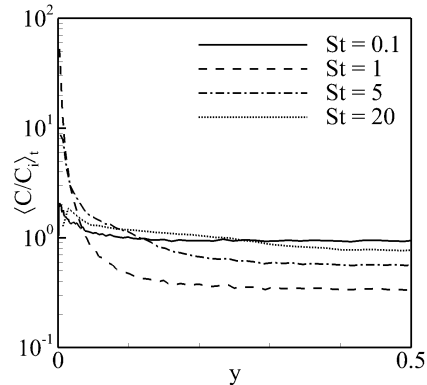


Figure 3. Time averaged particle concentration at Stokes number 0.1, 1, 5, 20.

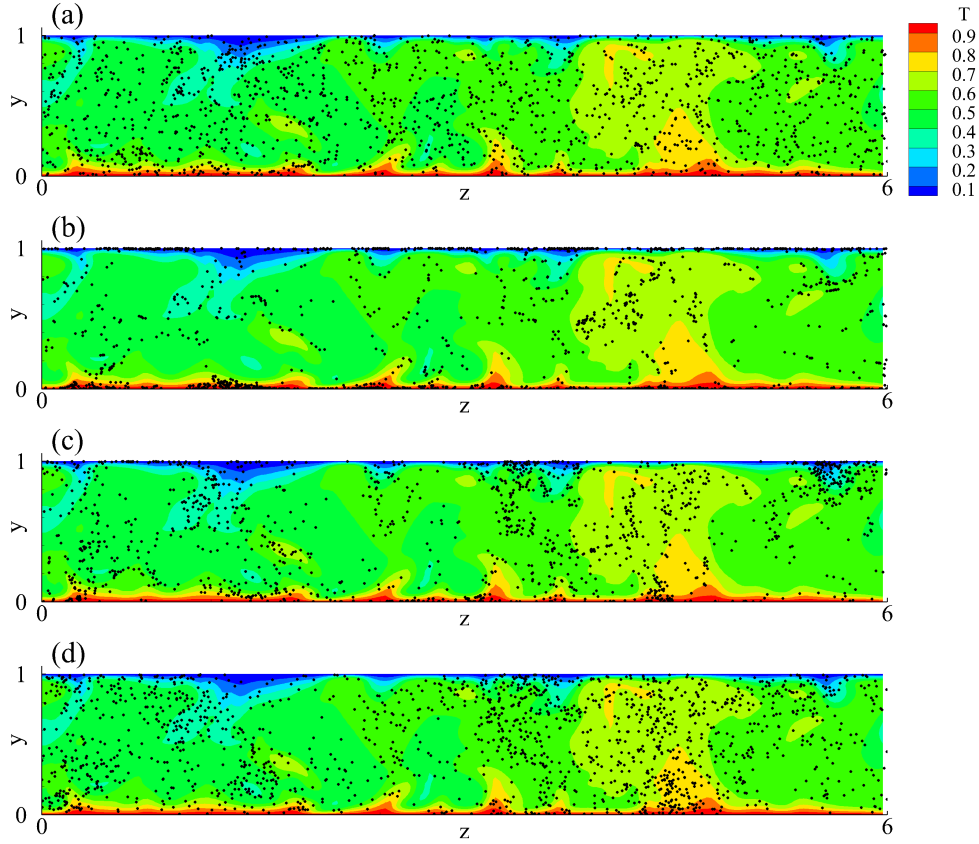


Figure 4. Side view of contour of temperature and particle distribution at  $x = 3$  when Stokes numbers are (a) 0.1, (b) 1, (c) 5 and (d) 20.

case, differences of particle concentration about vertical locations are not large compared to Stokes numbers 1 and 5, because particles do not respond quickly enough to follow the fluid motion. Figure 3 is time averaged particle concentration in the vertical direction, after the concentrations reached steady state ( $t^* > 250$ ), where  $t^*$  is normalized by domain height,  $H$ , and free fall velocity,  $U_f = \sqrt{\beta g H \Delta T}$ . As the figure shows, particle accumulation near the wall region is largest at Stokes number 1 case. On the other hand, almost uniform distributions are shown in Stokes number 0.1 and 20 cases.

Figure 4 indicates how particle distributions are affected by temperature and thermal plumes. As explained, distribution of Stokes number 1 particles are affected most, therefore particles are accumulated near the wall and they move horizontally by the horizontal flow in the region. Particles near the wall are often erupted by the vertically moving thermal plumes, which is shown by the alignment of particles with vertically stretched temperature contours at mixing and central regions (the red and blue colored area). Compared with Stokes number 1 and 5 cases, other cases of small and large Stokes number show relatively uniform distribution of particles, indicating that particles are not affected by thermal plumes as much as Stokes number 1 and 5 cases.

Figure 5 illustrates temperature contour and particle distribution at  $y = 0.012$ , near the wall when Stokes numbers are 0.1 and 1. The figure shows how particles concentrate at a plane of fixed vertical location. In Rayleigh-Bénard convection, horizontally moving sheet-like thermal

plumes are dominant, therefore fluid and particles converge to large temperature region, the red colored region in figure 5 (b). However, small Stokes number case is not affected by thermal structure as Stokes number 1 case.

In one-way coupling assumption of particle simulation, particles are only affected by flow structures, and thus the thermal plume, the dominant coherent structure, determines the particle motion in Rayleigh-Bénard convection. As studied by previous researchers about particle motions in turbulence, particles filter small scale motions of fluid depending on Stokes number, which is also shown in our simulation results.

## Conclusion

Different flow characteristics of regions in Rayleigh-Bénard convection are shown by velocity gradient tensor. Near the wall, sheet-like thermal plumes move horizontally due to wave propagation caused by the thermal plumes coming from the opposite side of the wall. At the flow converging region near the wall, hot/cold fluid is erupted and accelerated at the mixing layer. The invariant of velocity gradient tensor at mixing layer and central region shows pear-shape which is similar to isotropic turbulence, because central region behaves like nearly isothermal flow.

The dominant coherent structures that determine accumulation of particles in the Rayleigh-Bénard convection is thermal plumes. By converging and spreading at near-wall region, thermal plumes cause nonuniform distribution of particles. The acceleration of thermal plumes at mix-

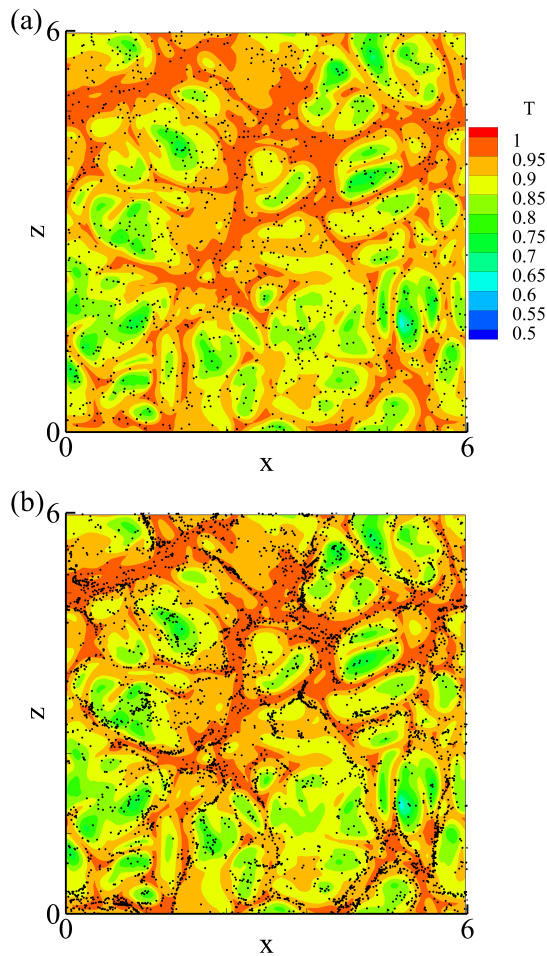


Figure 5. Contour of temperature and particle distribution at  $y = 0.012$  for Stokes number (a) 0.1 and (b) 1.

ing layer make particles move vertically, while mixing at central region make particle distribution relatively uniform. Depending on Stokes number, particle distribution shows different aspects. We showed that particle concentration is highly correlated with temperature when Stokes number is of order 1, clearly suggesting that particles are dominantly affected by thermal plumes in Rayleigh-Bénard convection.

## REFERENCES

- Blackburn, H. M., Mansour, N. & Cantwell, B. J. 1996 Topology of fine-scale motions in turbulent channel flow. *Journal of Fluid Mechanics* **310**, 269–292.
- Elghobashi, S. 1994 On predicting particle-laden turbulent flows. *Applied Scientific Research* **52**, 309–329.
- Elperin, T., Kleeorin, N. & Rogachevskii, I. 1996 Turbulent thermal diffusion of small inertial particles. *Physical Review Letters* **76**, 224.
- Krishnamurti, R. & Howard, L. N. 1981 Large scale flow generation in turbulent convection. *Applied Physics and Mathematical Sciences* **78**, 1981–1985.
- Ooi, A., Martin, J., Soria, J. & Chong, M. S. 1999 A study of the evolution and characteristics of the invariants of the velocity-gradient tensor in isotropic turbulence. *Journal of Fluid Mechanics* **381**, 141–174.
- Oresta, P., Lippolis, A., Verzicco, R. & Soldati, A. 2006 Dispersion and deposition of particles in rayleigh-bénard turbulent flows. In *Proceedings of FEDSM2006*, pp. 1703–1713. Miami, Florida.: ASME.
- Oresta, P. & Prosperetti, A. 2013 Effects of particle settling on rayleigh-bénard convection. *Physical Review E* **87**, 063014.
- Pallares, J. & Grau, F. X. 2012 Particles dispersion in a turbulent natural convection channel flow. *Journal of Aerosol Science* **43**, 45–56.
- Rouson, D. W. I. & Eaton, J. K. 2001 On the preferential concentration of solid particles in turbulent channel flow. *Journal of Fluid Mechanics* **428**, 149–169.
- Shishkina, O. & Wagner, C. 2006 Analysis of thermal dissipation rates in turbulent rayleigh-bénard convection. *Journal of Fluid Mechanics* **546**, 51–60.
- Shishkina, O. & Wagner, C. 2007 Local heat fluxes in turbulent rayleigh-bénard convection. *Physics of Fluids* **19**, 51–60.
- Shishkina, O. & Wagner, C. 2008 Analysis of sheet-like thermal plumes in turbulent rayleigh-bénard convection. *Journal of Fluid Mechanics* **599**, 383–404.
- Soldati, A. 2005 Particles turbulence interactions in boundary layers. *Journal of Applied Mathematics and Mechanics* **85**, 683–699.
- Zocchi, G., Moses, E. & Libchaber, A. 1990 Coherent structures in turbulent convection, an experimental study. *Physics A* **166**, 387–407.